Light scattering and fluorescence studies of block copolymer micelles of polystyrene-*block*-poly(hydrogenated isoprene) in the selective solvent 1,4-dioxane-n-heptane

Karel Procházka*
Department of Physical Chemistry, Faculty of Science, Charles University in Prague, Albertov 2030, 128 40 Prague 2, Czechoslovakia

and Bo Medhage, Emad Mukhtar and Mats Almgren
Department of Physical Chemistry, Uppsala University, PO Box 532, S-751 21 Uppsala, Sweden

and Petr Svoboda, Jitka Trněná and Bohumil Bednář
The Prague Institute of Chemical Technology, Prague 6, Czechoslovakia
(Received 14 February 1992)

Diblock polystyrene-*block*-poly(hydrogenated isoprene) was fluorescence labelled by random covalent attachment of anthracene at the polystyrene block (the average number of anthracenes per copolymer chain was 0.88). Micellization of the labelled copolymer was studied in a broad composition range of the solvent mixture 1,4-dioxane/heptane. Micelles with polystyrene cores are formed in heptane-rich solvents (0–30 vol% 1,4-dioxane). In mixtures with 30–50 vol% 1,4-dioxane, the sample dissolves molecularly in the form of individual copolymer coils and in dioxane-rich solvents (more than 50 vol% 1,4-dioxane), micelles with polystyrene shells are formed. Micellar solutions were characterized by static and quasielastic light scattering and by sedimentation velocity measurements. The mobility of pendant fluorophores and polymer segments in micellar cores and shells in selective solvents and in individual copolymer coils in good solvents was studied by time-resolved fluorescence-anisotropy measurements.

(Keywords: block copolymer micelles; selective solvent/precipitant; static and quasielastic light scattering; ultracentrifugation; steady-state and time-resolved fluorescence; fluorescence anisotropy; dynamics and mobility of polymer segments)

INTRODUCTION

The behaviour of block copolymers differs strongly in many respects from that of both homopolymers and random copolymers. In selective precipitants (or selective solvents), i.e. precipitants for one block and good solvents for the other block, minimization of unfavourable interactions of insoluble block segments with solvent molecules, together with a reasonable entropy balance of the system, result in the formation of multimolecular micelles[1–3] with a relatively high association number (tens to hundreds of associated polymer chains). Multimolecular block copolymer micelles contain very dense spherical cores (segment density $\sim 0.7-0.8\ g\ cm^{-3}$) formed from the insoluble blocks, and diffuse outer shells (coronas) formed from the soluble blocks.

Micellization of block copolymers in dilute solutions in selective precipitants has been studied by various experimental techniques[1–3] over the past few decades. It has been shown that this process obeys the scheme of a closed association[4], characterized by a reversible equilibrium:

$$nU \overset{K}{\rightleftharpoons} M \qquad (1)$$

where U represents unimers (non-micellized, molecularly dissolved copolymer chains), M represents micelles, n is the association number and K is the equilibrium constant. The micelles are usually nearly monodisperse in mass and size. The association number, n, depends on copolymer composition, solvent quality and temperature; the unimer-to-micelle mass ratio varies further with total copolymer concentration according to the mass action law (equation (1)) for concentrations above the critical micelle concentration (CMC); below CMC only unimer molecules are present.

In spite of extensive experimental data on the micellization equilibrium, little is known concerning the dynamics of unimer–micelle mass exchange under equilibrium conditions. Indirect data from size exclusion

* To whom correspondence should be addressed

0032-3861/93/010103-08

chromatography (s.e.c.)[5,6] along with sedimentation velocity measurements[7] indicate that the association/dissociation may be relatively fast (at least on the timescale which may be distinguished by using those methods, i.e. 10^{-2}–10^{1} s). Stopped flow measurements[8] confirmed the important role of the copolymer structure (number of blocks etc.) mainly in the case of dissociation dynamics. It must be kept in mind, however, that the stopped flow data refer to a large perturbation of the equilibrium and do not describe the equilibrium mass exchange.

Direct experimental data[9] concerning the copolymer chain release and its incorporation into a micelle under equilibrium conditions show that in less selective precipitatnts, where the micellar core is swollen, the mass exchange rate is high. The dynamics of the association/dissociation process are influenced mainly by the segmental motion of the insoluble blocks in the micellar cores and their disentanglement.

The dynamics of polymer segments may be studied either by n.m.r.[10–13], or, for a copolymer labelled by a fluorescent marker, by time-resolved fluoresence techniques[14]. The rotation of a pendant fluorescent group attached covalently to the polymer chain provides indirect information on the polymer chain dynamics and possible structural changes of the host system.

With the advent of subnanosecond time-resolved fluorescence depolarization techniques in recent years, studies of polymer chain dynamics have become more frequent[15–18], but results on block copolymer micelles are still scarce[19,20].

The aim of this work is to study the micellization of the fluorescently tagged block copolymer polystyrene-*block*-poly(hydrogenated isoprene) in a broad range of compositions of the mixed solvent 1,4-dioxane/n-heptane by various techniques. Special attention is given to the relationship between the mobility of the pendant fluorescent groups and the compactness of the micellar core in solvents with varying solvent selectivity.

EXPERIMENTAL

Materials

Polymers. The fluorescence-labelled diblock copolymer sample of polystyrene-*block*-poly(hydrogenated isoprene) (A-SHI) was a purified fraction of Kraton G1701 ($M_w = 1.03 \times 10^5$ g mol^{-1}, weight fraction of polystyrene $x_S = 0.42$, narrow distribution of molar masses) tagged with anthracene. Anthracene was covalently attached to the aromatic ring of polystyrene via a $-CH_2-O-CH_2-$ bridge. First, 9-anthraldehyde was synthesized[21], then it was reduced to 9-anthracenemethanol[22]. The polystyrene block was chlormethylated[23] to a low degree and the tagging was achieved by reacting the potassium salt of 9-anthracenemethanol with the chlormethyl group[24]. The tagging was random and the average number of anthracene fluorophores per chain was 0.88. The weight average molar mass and molar mass distribution of A-SHI were measured after tagging and purification and remained the same, within experimental errors, as in the original G1701 fraction.

Anthracene-tagged anionic polystyrene (A-PS) was prepared and characterized by light scattering ($M_w = 5.1 \times 10^3$ g mol^{-1}), s.e.c. ($M_w/M_n < 1.2$) and by u.v.–vis. absorption spectroscopy (average content, 0.76 anthracene fluorophores per chain).

Solvents. 1,4-Dioxane and n-heptane, both for u.v. spectroscopy, were used as purchased (Aldrich).

Methods

Static light scattering. Static light scattering measurements were performed using a Sofica 42000 apparatus with vertically polarized light ($\lambda = 546$ nm) within the angle range 30–150°. The values of the relative scattered light intensity, $I_{rel} = (I - I_0)/I_0$, extrapolated to zero scattering angle were used to evaluate the micellar molar mass. I and I_0 are the intensities at a low micelle concentration ($\sim 1 \times 10^{-3}$–4×10^{-3} g cm^{-3}) and for the solvent, respectively. I_{rel} is proportional to the apparent weight average molar mass, $M_w^{(app)}$, of all polymer particles (unimer coils and micelles) in a solution:

$$M_w^{(app)} = w_U M_U + w_M M_M \quad (2)$$

where w_U and w_M are weight fractions and M_U and M_M are weight average molar masses of unimers and micelles, respectively. For systems where the micelles contain tens of copolymer chains and the micellization equilibrium is shifted in favour of the micelles, $M_w^{(app)}$ and M_M are close to each other. Refractive index increments at the osmotic equilibrium of low molar mass components in the solution were measured as described elsewhere[25].

Quasielastic light scattering. The apparent hydrodynamic radii, R_H, of unimer and micelles (at low, but finite concentration) were measured using a Brookhaven BI 2030 apparatus with a 72-channel correlator in the angle range 30–150°. A He-Ne laser ($\lambda = 632.8$ nm) was used as a light source. The self-beating autocorrelation function was measured:

$$g^{(1)}(q, t) = \exp[-\Gamma(q)t + 0.5\mu_2(q)t^2 + \cdots] \quad (3)$$

where q is the scattering vector and t is the sampling time. The diffusion coefficient, D, and R_H were calculated from the first cumulant, $\Gamma(q)$:

$$D = \Gamma(q)/q^2 \quad (4)$$

$$R_H = kT/6\pi\eta_0 D \quad (5)$$

where k is the Boltzmann constant, T is the temperature and η_0 is the solvent viscosity. The polydispersity in diffusion coefficients, $P_D = \mu_2(q)/\Gamma(q)^2$ (where μ_2 is the second cumulant) was small for systems where either micelles or unimers are dominant ($P_D \approx 0.02$–0.03), but rose to 0.2–0.3 in systems containing comparable weight fractions of both components. Since the values obtained from quasielastic light scattering correspond to the z-average diffusion coefficient, $\langle D \rangle_z$, and the molar mass of the micelles is much higher than that of the unimer, the measured values are very sensitive to the presence of micelles in the solution. Once micelles are present, the experimental values of R_H approach the expected values of micelles, even in solutions with a high content of unimer.

Ultracentrifugation. The sedimentation velocity measurements were performed with a MOM 3107 analytical ultracentrifuge (Hungary) with Schlieren optics as described elsewhere[7]. The sedimentation velocity diagrams of reversibly associating micellar systems were interpreted on the basis of the Gilbert theory[26].

Fluorescence measurements. Steady-state spectra were recorded using a Spex Fluorolog 212 spectrometer (Spex Ind., NJ, USA). The samples were excited in the spectral region 326–390 nm and the emission was detected at 416 nm. Glan-Thompson u.v. polarizers were used on the excitation and emission side to measure the parallel intensity $I_{\parallel}^{ss}$ and the perpendicular intensity $I_{\perp}^{ss}$.

Time-resolved measurements. Fluorescence decay data were collected using the time-correlated single photon counting technique with a synchronously pumped and cavity dumped DCM dye laser with frequency doubling. The experimental details have been given elsewhere[9].

The excitation polarization was adjusted to be vertical by means of a Soleil-Babinet compensator. The emission was monitored through a polarizer with orientation either parallel, perpendicular or at the magic angle (54.7°) relative to the excitation polarization.

True polarized fluorescence decay curves, i.e. functions free from convolution effects, are given by:

$$i_{\parallel}(t) = \tfrac{1}{3}F(t)[1 + 2r(t)] \quad (6)$$

$$i_{\perp}(t) = \tfrac{1}{3}F(t)[1 - r(t)] \quad (7)$$

where $F(t)$ represents the photophysics and $r(t)$ the anisotropy decay. Both $F(t)$ and $r(t)$ are described by sums of exponentials:

$$F(t) = \sum_{i=1}^{n_F} \alpha_i e^{-(t/\tau_i)} \quad (8)$$

$$r(t) = \sum_{i=1}^{n_r} r_i e^{-(t/\phi_i)} \quad (9)$$

A scaling factor, G, was used in the analysis to account for differences in data acquisition times, polarization dependence of the microchannel plate detector and the monochromator, geometrical factors, etc. This factor was calculated by normalizing the total number of counts $I_{\parallel}$ and $I_{\perp}$, collected in the decay curves $I_{\parallel}(t)$ and $I_{\perp}(t)$ respectively, to the measured steady-state anisotropy, $\langle r \rangle$.

$$G = \frac{1 - \langle r \rangle}{2\langle r \rangle + 1} \frac{I_{\parallel}}{I_{\perp}} \quad (10)$$

Parallel- and perpendicular-polarized decay curves were fitted simultaneously by a non-linear least-squares program using a modified Levenberg–Marquardt algorithm with iterative reconvolution[27–31]. Also included in the analysis was a time shift parameter, originating from a small inevitable mismatch in the positioning of the instrumental response function (measured with a scattering solution) relative to the fluorescence decays, mainly due to quantization and wavelength effects. The shift parameter was always found to be less than the width of one time channel (20.6 ps).

RESULTS AND DISCUSSION

Characterization of micellar solutions

Characterization of micellar solutions and determination of borders between good and selective solvents were performed by light-scattering techniques. The results are summarized in *Figure 1*. Curve a shows the apparent molar mass, $M_w^{(app)}$, corresponding to all polymer particles in a solution as a function of solvent composition. Heptane-rich solvents are selective precipitants for polystyrene. Multimolecular micelles with polystyrene cores are formed and the measured values of $M_w^{(app)}$ are very high. A fast decrease in $M_w^{(app)}$ with increasing content of 1,4-dioxane is observed as 1,4-dioxane improves the solubility of polystyrene blocks. In mixtures containing 0–15 vol% 1,4-dioxane, the micellization equilibrium is significantly shifted towards the micelles (especially at high copolymer concentration, $c = 0.5–1.0 \times 10^{-2}$ g cm^{-3}). Only one fast sedimenting peak was obtained in sedimentation measurements in these solvents (results not shown here), whereas in mixtures with 15–30 vol% of 1,4-dioxane, two peaks were observed, and in very mild selective precipitants (around 20–30 vol% 1,4-dioxane), the measured curve between the two peak maxima did not fall to the baseline, which indicates a mobile association/dissociation equilibrium[26]. At low copolymer concentrations, a small fraction of unimer was also detected in mixtures with a lower 1,4-dioxane content (in the region around 10 vol% of 1,4-dioxane). Mixtures containing 30–50 vol% of 1,4-dioxane are good solvents for both blocks. The measured values of $M_w^{(app)}$ correspond to those of unimers in a good solvent (e.g. tetrahydrofuan or toluene) and only one slowly sedimenting species was detected by ultracentrifugation. 1,4-Dioxane-rich mixtures are selective precipitants for hydrogenated polyisoprene, and micelles with aliphatic cores and polystyrene shells are formed, accompanied by a steep increase in $M_w^{(app)}$. Mixtures with more than 70 vol% of 1,4-dioxane are very strong selective precipitants for aliphatic polymers, and the presence of unimers was precluded by sedimentation velocity measurements.

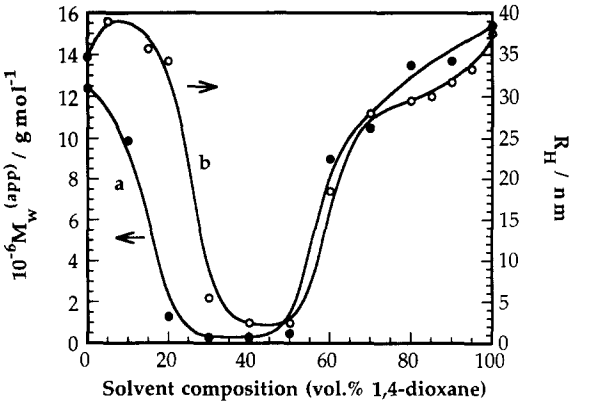

Figure 1 Apparent molar mass, $M_w^{(app)}$ (curve a), and apparent hydrodynamic radius, R_H (curve b), of the micellizing diblock polystyrene-*block*-poly(hydrogenated isoprene) sample A-SHI in a selective precipitant mixture 1,4-dioxane/heptane as a function of the solvent composition, $T = 298$ K

Curve b in *Figure 1* shows the apparent hydrodynamic radius R_H as a function of solvent composition. The conclusions drawn from the quasielastic light scattering measurements agree with those obtained by static light-scattering, which is evident from comparison of both curves.

Light-scattering data indicate that in both heptane-rich and 1,4-dioxane-rich solvents, the micelles contain more than 100 unimers and their R_H is in the region 30–40 nm. The average segment density is quite high (0.15–0.18 g cm^{-3}), which is in agreement with the data for common copolymer systems[1–3]. It must be kept in mind, however, that the $M_w^{(app)}$ data represent apparent values only, and the light scattering measurements[32] for

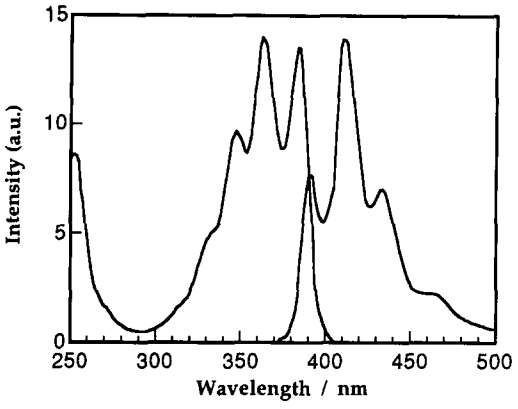

Figure 2 Steady-state excitation and emission spectra of the anthracene-labelled copolymer A-SHI in cyclohexane

G1701 in aliphatic solvents give negative apparent radii of gyration R_g, which has not yet been explained to our knowledge.

Time-resolved fluorescence measurements

In order to obtain information on micellar compactness and segmental motions in micellar cores, time-resolved fluorescence measurements were performed. The arrangement and the local motion of segments in the close vicinity of a pendant label affect its rotational freedom. Rotational diffusion of labels can be monitored by time-resolved anisotropy measurements.

The steady-state excitation and emission spectra of the anthracene-labelled copolymer in cyclohexane are shown in *Figure 2*. They are similar to those of pure anthracene in cyclohexane; only a small red shift of ~5 nm may be observed.

The fluorescence decays of the labelled copolymers in solvent mixtures were generally non-exponential, which is quite common for polymer systems[33]. Satisfactory fits required triple-exponential functions. For all the solvent compositions studied the three-exponential photophysics has a major (~80%) component of about 2 ns and two minor (10–20% and 5–10%) components of 0.5–1 ns and 4–5 ns, respectively. The experimental fluorescence decays of pure anthracene in all solvents were single-exponential (in heptane the fluorescence lifetime was found to be 3.54 ns). This behaviour indicates that the interactions of the labels with surrounding chain segments and with solvent molecules are quite complex and that the microenvironment of individual labels in a given macroscopic solution is non-homogeneous (mainly due to a random attachment of labels to individual chains). However, it was not the aim of this work to study these effects in detail. Typical decay curves of fluorescence-labelled copolymers in several solvent mixtures are shown in *Figure 3*.

It should be remarked that equations (6) and (7) are valid under the assumption that the fluorescence and the anisotropy decays are independent. If the complex photophysics of the anthracene label is due to labels in different environments, then a coupling between the photophysics and the reorientation could be suspected. That would mean that equations (6) and (7) should be replaced by sums over all microenvironments, so that:

$$i_\alpha(t) = \tfrac{1}{3}\sum_i F_i(t)[1 + (3\cos^2\alpha - 1)r_i(t)] \quad (11)$$

where α represents the polarizer angle. Such complications are, of course, impossible to handle with reasonable reliability, especially in the present case since the information available was diminished by the internal depolarization as described below.

Two sets of time-resolved fluorescence depolarization measuremets were performed on the system under study:

1. Measurements with an Edinburgh 299T fluorometer for excitation at 380 nm (close to the 0–0 transition). Most of the data, as well as the experimental details, have been reported earlier[19,20]. The time-resolution was, however, not high enough to allow a precise determination of the short depolarization times. Nevertheless a relatively simple photophysics of anthracene for this excitation wavelength (without a significant internal depolarization of the probe, see below) made it possible to obtain quite accurate values of the residual anisotropy, r_∞.
2. In this study, measurements with much better time resolution were performed (see Experimental section). An excitation wavelength, λ, of 326 nm was chosen, which was a compromise between the excitation span of the apparatus and the spectral properties of the labelled copolymer. The experimental set-up did not permit us to excite in the spectral region 350–400 nm, where the most intense absorption bands of anthracene are located. The necessity to excite at 326 nm caused a number of problems and diminished the information gained by the anisotropy measurements. The results obtained have shown that the anisotropy data must be interpreted with great care and precaution, when an anthracene label is used.

In the polarization spectra of anthracene, there is a strong overlap of the absorption bands polarized in the direction of the long and short symmetry axis of the molecule in the spectral region 320–390 nm[34]. As a consequence, there is a significant intermixing of excited vibrational states of vibrations with different symmetries and a fast partial depolarization takes place. This depolarization proceeds on a picosecond timescale, and in our experiments the short depolarization correlation times 10–30 ps correspond mainly to this process. The observed times represent an upper estimate of the shortest depolarization time limit obtainable with the instrument.

It has been shown by measuring the steady-state anisotropy, $\langle r \rangle$, in supercooled systems containing

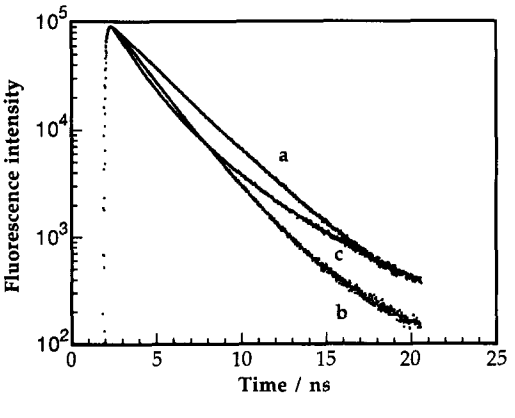

Figure 3 Magic angle fluorescence decay curves for the anthracene-labelled copolymer A-SHI in heptane (curve a), 1,4-dioxane (curve b) and the mixture heptane/50 vol% 1,4-dioxane (curve c), copolymer concentration $c = 1 \times 10^{-2}$ g cm^{-3}

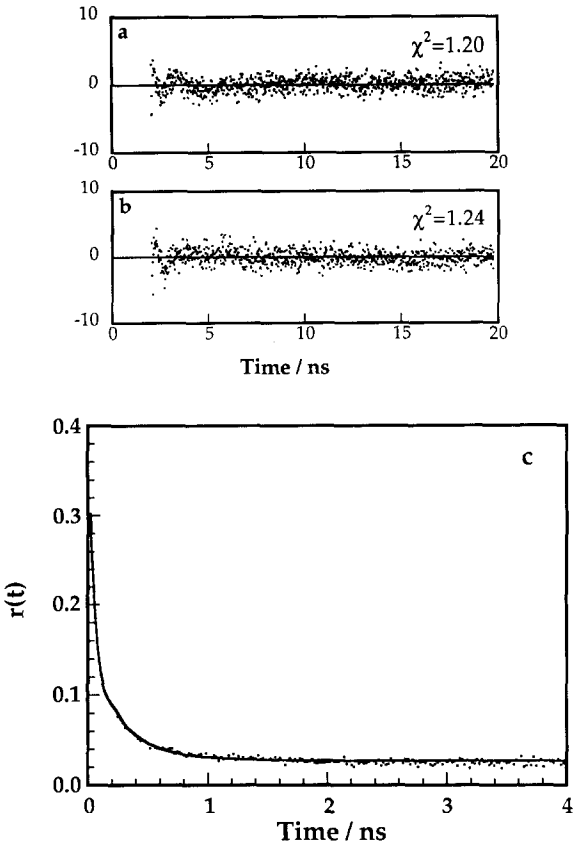

Figure 4 (a) and (b) The quality of a fit illustrated by plots of the weighted residuals obtained from the simultaneous analysis of parallel and perpendicular decay curves, respectively. $\chi^2_{global} = 1.22$. (c) Point-by-point fluorescence anisotropy calculated from $r(t) = [I_{\parallel}(t) - GI_{\perp}(t)]/[I_{\parallel}(t) + 2GI_{\perp}(t)]$, hence, without respect to convolution or time-shift effects. The peak channel in the instrumental response function was chosen to define $t = 0$. All data correspond to the anthracene-labelled copolymer in heptane, copolymer concentration $c = 1 \times 10^{-2}$ g cm^{-3}

anthracene derivatives[35], that the contribution of the internal depolarization increases with decreasing excitation wavelength. Our experiments indicate that for the excitation at 326 nm, the fast depolarization mechanism contributes ~85% to the total depolarization, and thus reduces the information on the rotational diffusion and on other types of reorientational motion. The high-time resolution of the apparatus (~20 ps per channel), the narrow excitation profile and the fast response of the detector (the half-width of the instrumental response function was ~80 ps) together with the very high number of counts in the peak channel (always $> 10^5$) partially compensate for this considerable drawback.

The time-resolved anisotropy decays were obtained on the basis of simultaneous analysis of polarized fluorescence data. To fit the polarized decay curves, a double exponential function with a residual term was used to describe the anisotropy decay. As mentioned earlier, the short correlation time, ϕ_1, corresponds essentially to the so-called parasite effect caused by the complicated photophysical properties of anthracene labels, and the longer correlation time, ϕ_2, describes mainly the reorientational motion of the pendant groups and in some cases other possible depolarization processes (e.g. energy transfer, see the discussion below). In the case of a labelled copolymer in a good solvent, it is mainly a one-dimensional rotational diffusion with respect to the axis formed by the covalent bond connecting the label to the polymer chain. This rotational motion may be further accompanied by a slower segmental motion and reorientations of certain parts of the polymer chain (depending on the flexibility of the polymer chain, thermodynamic interactions, etc).

Typical weighted residuals obtained from a simultaneous analysis of polarized fluorescence decay curves are shown in *Figure 4* together with the constructed point-by-point anisotropy, $r(t)$ (solvent, heptane; copolymer concentration, $c = 1 \times 10^{-2}$ g cm^{-3}). The upper estimate of the fast depolarization time is $\phi_1 = 12 \pm 5$ ps. Similar upper estimates of ϕ_1 were reached in the other measurements.

The long reorientational correlation time was $\phi_2 = 250 \pm 90$ ps. The relatively high standard deviation was caused by the small contribution of the reorientational motion to the overall depolarization. We did not attempt to fix the initial anisotropy to the theoretical value, $r_0 = 0.4$, for the parallel orientation of absorption and emission transition moments to each other. For solvents with 0–50 vol% of 1,4-dioxane, the pre-exponential factors r_1 were in the range 0.30–0.35 and r_2 in the range 0.05–0.08, so that the value $r_0 = 0.4$ was roughly fulfilled. Due to the complicated photophysics of anthracene, this value is not relevant and the most important characteristic of the fluorophore is the roughly constant value r_2, which represents the 'initial' anisotropy after vibrational relaxation.

Before any detailed discussion of the time-resolved polarization fluorescence data with respect to the polymer structure and possible motions of the polymer chain and pendant groups, it should be stressed that, in the absence of energy transfer, ϕ_2 represents an effective reorientational correlation time, describing a complex motion of labels for an ensemble of all simultaneous arrangements of polymer chains in a given solution. Because of the high internal depolarization of anthracene labels for the excitation at 326 nm, it was not possible to distinguish more than one correlation time (and a residual anisotropy) for the true reorientational modes.

In *Figure 5* the effective reorientational times, ϕ_2, are plotted as a function of the solvent composition. For further discussion, we shall divide the solvent mixtures into three classes.

Good solvents for both blocks. In solvents containing

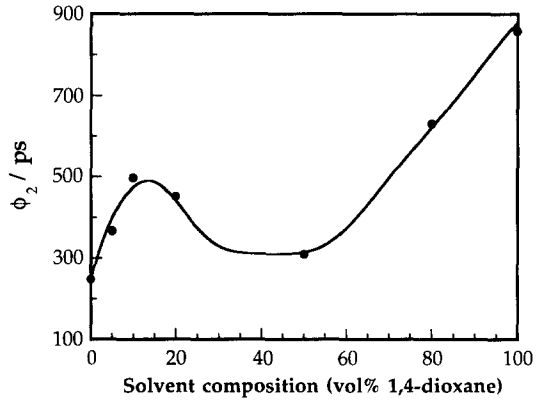

Figure 5 Reorientation correlation times, ϕ_2, *versus* solvent composition for the anthracene-labelled copolymer A-SHI. Copolymer concentration $c = 1 \times 10^{-2}$ g cm^{-3}, $T = 298$ K

30–50 vol% of 1,4-dioxane, the copolymer sample dissolves in the form of individual polymer coils. The density of segments as a function of the distance from the centre of gravity is similar to a Gaussian distribution. Coils are expanded by solvent molecules and the average density within a polymer coil is ~ 0.03 g cm^{-3}. Individual fluorescent labels are free to rotate and the motion of the polymer chain is relatively fast and easy. The curve ϕ_2 *versus* solvent composition shows a minimum in this region. The residual anisotropies, r_∞, approach zero within the range of experimental errors (for 50 vol% of 1,4-dioxane, $r_\infty = 0.003 \pm 0.003$ for excitation at 326 nm and $r_\infty = 0.01 \pm 0.02$ for excitation at 380 nm), indicating a relatively fast three-dimensional depolarization (i.e. not only the rotation of a pendant fluorophore along the axis, which is represented by a single covalent bond connecting the fluorophore to the polymer chain, but also the moderately fast motion of a part of the polymer chain involving this bond). The rotation correlation time $\phi_2 \approx 300$ ps is significantly longer than that of pure anthracene in a non-viscous solvent[36] ($\phi = 17 \pm 2$ ps for anthracene in dimethyl ether), which is fully understandable. The rotation of the pendant anthracene label is slowed down firstly due to chemical bonding to the polymer chain, and secondly due to the higher microviscosity of the microenvironment—the rotation is hindered by relatively rigid (as compared to solvent molecules) polymer segments, which may come into close proximity with the anthracene as a consequence of a moderately fast segmental motion.

Selective precipitant for the labelled polystyrene block. In heptane-rich solvents, the labels are either trapped in dense and compact polystyrene cores, or located in relatively contracted polystyrene blocks in unimer coils. In very strong selective precipitants, the equilibrium is shifted in favour of micelles, whereas in mild selective precipitants, a significant percentage of the copolymer may exist as unimer (mainly in very dilute solutions). In that case, the micellar cores are swollen[9] by solvent (mainly by 1,4-dioxane), as a consequence of the preferential sorption of the better solvent component[25]; the polystyrene blocks in unimers are also less contracted.

In unimers, the rotational motion is hindered due to the contraction of the unimer coil (as compared with the good solvent). In swollen micellar cores, a relatively slow and hindered rotational diffusion of pendant groups is possible[20,37]. As a consequence, the effective value ϕ_2 is increasing in mild selective precipitants for polystyrene (30–20 vol% of 1,4-dioxane) as compared to that in good solvents. For the copolymer concentrations studied, a significant fraction of unimer is present only in extremely mild selective precipitants of either block (close to the onset of micellization, around 30 vol% 1,4-dioxane for micelles with polystyrene cores).

In stronger selective precipitants for polystyrene (10–20 vol% of 1,4-dioxane), the rotation of the bulky pendant fluorophores becomes more hindered and as the compactness of the cores increases (0–10 vol% of 1,4-dioxane), the rotation is no longer possible and only relatively fast, but restricted, torsional vibrations partially depolarize the fluorescence emission. As a consequence the effective correlation time decreases, while the residual anisotropy increases (for 0 vol% of 1,4-dioxane, $r_\infty = 0.035 \pm 0.007$ for excitation at 326 nm and $r_\infty = 0.3 \pm 0.04$ for excitation at 380 nm).

In micelles with compact cores, a large number of fluorophores are located in a small volume relatively close to each other. There exists then a possibility of electronic energy transfer among the anthracene molecules and a subsequent complicating contribution to the depolarization (depending on the spatial and orientational distribution of the fluorophores). Energy transfer in polymer systems and its influence on the fluorescence decay, as well as on the time-resolved anisotropy, has been studied by many workers, in particular by Fayer and co-workers[38–41] and by Frank and co-workers[42,43]. It has been found that in some systems the depolarization due to energy transfer is quite important. It has also been shown that in systems of immobilized fluorophores the depolarizing contribution from energy transfer is less important than in a system where the probes rotate fast[42,43].

Micellar systems of polystyrene-*block*-hydrogenated polyisoprene have been studied by SAXS by Tuzar *et al.*[44] and it was found that the segment density in the micellar cores in strong selective solvents is ~ 0.7–0.8 g cm^{-3}. Such values are generally assumed to be typical core densities for non-polar block copolymer micelles in organic selective solvents[1–3]. In our system the hydrodynamic radius of the micelle, R_H, in heptane-rich solvents was ~ 35 nm. A reasonable estimation of the core radius, $R_{core} \approx 15$ nm, leads to the following densities: $\rho_{core} = 0.71$ g cm^{-3} and $\rho_{shell} = 0.12$ g cm^{-3}, which correspond well to the literature data. The average distance between fluorophores in a core with a radius of ~ 15 nm would be ~ 46 Å (for our density of labels per chain), which is considerably larger than the Förster radius, $R_0 = 22$ Å for anthracene[45].

So far very little is known about the true distribution of individual blocks within micellar cores. Both theoretical[46–48] and experimental[49] studies focus mainly on the distribution of the free ends of blocks grafted to the concave spherical surface. The results are often contradictory and the conclusions are not generally comprehensive; nevertheless it seems that the distribution of individual blocks is quite uniform within the core. In our systems, where the labelling of individual blocks is low and random, we can assume quite a uniform spatial distribution of fluorophores (since the combination of two random and statistically uncorrelated events, i.e. the chemical attachment of a label to a chain and the spatial distribution of individual blocks in the core, should lead to a uniform spatial distribution of labels in the core).

The high values of the residual anisotropies and the steady-state anisotropies for excitation at 380 nm indicate that the depolarization due to energy transfer is not very important in the studied systems. However, a small effect of energy transfer, in part due to the possible clustration tendency of the anthracenes (and to the small fraction of randomly distributed fluorophore pairs with the interfluorophore distance comparable to the Förster radius, R_0) cannot be completely ruled out. The conclusions concerning the restricted motion of the fluorophores would be correct even in the case of a small energy transfer contribution. The reorientational depolarization would be more limited in that case.

Selective precipitant for hydrogenated polyisoprene. In 1,4-dioxane-rich solvents, micelles with polystyrene shells are formed. The average segment density (~ 0.10–

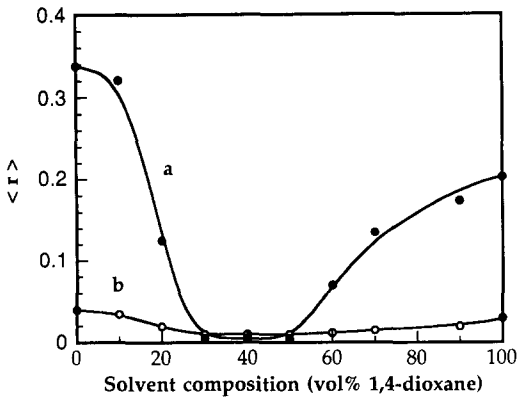

Figure 6 The steady-state anisotropies of the anthracene-labelled block copolymer in a solvent mixture as a function of the solvent composition. Copolymer concentration $c = 1 \times 10^{-2}$ g cm^{-3}, $T = 298$ K. Excitation wavelength = 385 nm (curve a), 326 nm (curve b)

0.20 g cm^{-3}) is significantly lower than in the micellar cores, but much higher than in individual polymer coils in a dilute solution. The shell region thus corresponds to a relatively concentrated polymer solution; however, the chains are partially organized (preferentially radially stretched). The segment density decreases from the core/shell interface towards the shell periphery. Due to the random attachments of labels to individual blocks, some fluorophores are closer to the core, where the microviscosity is high, whereas others are located at the shell periphery and experience lower microviscosity. Furthermore, the spatial distribution of the fluorophores in the shell region is not uniform either; the density decreases towards the shell periphery. The average segmental motion is slowed down as compared to the case of a single polymer coil in dilute solution in a good solvent. The inhomogeneity in the probe microenvironment may be the reason why the ratio r_1/r_2 is shifted in favour of the term r_1, and the short correlation time, ϕ_1, is considerably longer (40–60 ps) than in the previously discussed cases. It is possible that ϕ_1 in this case (in addition to the vibrational depolarization) also reflects some fast reorientational mode. The partial orientation of the polystyrene blocks (which are flexible, although they are radially stretched) in the shells prevents the reorientation from proceeding efficiently in all three directions and the residual anisotropy is non-zero ($r_\infty = 0.010$–0.014 for excitation at 326 nm and $r_\infty > 0.2$ for excitation at 380 nm).

To support the conclusions drawn from the time-resolved measurements, the steady-state anisotropies were measured for various excitation wavelengths. At first the steady-state anisotropy of an anthracene-labelled low molar mass polystyrene was measured in solid 1,4-dioxane. 1,4-Dioxane is a very good solvent for polystyrene with a high freezing temperature (4.5°C) and so it is possible to freeze the polystyrene solution without precipitating the polymer. Motions of polymer segments and pendant groups were frozen and no reorientational depolarization took place. For the excitation at 326 nm, the steady-state anisotropy, $\langle r \rangle$, was 0.04, whereas for the excitation at 385 nm the corresponding value was 0.34 (emission at 420 nm). These measurements are in full agreement with data of other authors[19] and indicate that the fast depolarization process (for the excitation at 326 nm) is a consequence of the photophysical properties of anthracene itself.

Secondly, the steady-state anisotropy for the labelled copolymer was measured in the whole range of solvent mixtures with excitation at both 326 nm and 385 nm, at the copolymer concentration $c = 1 \times 10^{-2}$ g cm^{-3}. The results are shown in *Figure 6*. The shape of the curve is very similar to those of $M_w^{(app)}$ or R_H *versus* solvent composition (*Figure 1*). With respect to the previous discussion, the curves need no further explanation; they add strength to the conclusions outlined above.

CONCLUSIONS

Time-resolved and steady-state fluorescence depolarization techniques are, especially in combination with light-scattering techniques, powerful tools in the study of polymer chain dynamics. Studies of the behaviour of fluorescent labels, covalently attached to polymer chains, seem able to provide valuable information on micellar compactness and chain dynamics in copolymer systems. Since the reorientational motion of a pendant probe in these systems typically takes place on a subnanosecond time-scale, picosecond time resolution is required to extract the desired information.

The results presented in this paper indicate that the reorientational motion of the pendant groups is very complex in systems for micellizing copolymers. A broader knowledge of the behaviour of the system (i.e. the light scattering and the ultracentrifugation data together with the data of other authors for similar systems) is necessary for the correct interpretation of the time-resolved anisotropy measurements.

The anthracene probe should be used with great care in fluorescence anisotropy studies, because of its internal depolarization properties, which may complicate the depolarization of the fluorescence considerably, depending on the excitation wavelength. Excitation of anthracene around 380 nm would minimize these problems and is strongly recommended in future studies.

ACKNOWLEDGEMENT

This work was supported by grants from the Swedish Natural Science Research Council.

REFERENCES

1 Tuzar, Z. and Kratochvil, P. *Adv. Colloid Interface Sci.* 1976, **6**, 201
2 Tuzar, Z. and Kratochvil, P. in 'Surface and Colloid Science Series' (Ed. E. Matijevic), Vol. 15, Plenum Press, New York, in press
3 Riess, G., Hurtrez, G. and Bahadur, P. in 'Encyclopedia of Polymer Science and Engineering' (Eds H. F. Mark, N. M. Bikales, C. G. Overberger and G. Menges), Vol. 2, 2nd edn, J. Wiley, New York, 1985, pp. 324–436
4 Elias, H.-G. *J. Macromol. Sci.* 1973, **A7**, 601
5 Prochazka, K., Mandak, T., Kocirik, M., Bednar, B. and Tuzar, Z. *J. Chem. Soc., Faraday Trans. 1* 1990, **86**, 1103
6 Prochazka, K., Mandak, T., Bednar, B., Trnena, J. and Tuzar, Z. *J. Liquid Chromatogr.* 1990, **13**, 1765
7 Prochazka, K., Gloeckner, G., Hoff, M. and Tuzar, Z. *Makromol. Chem.* 1984, **183**, 2521
8 Bednar, B., Edwards, K., Almgren, M., Tormod, S. and Tuzar, Z. *Makromol. Chem. Rapid Commun.* 1982, **3**, 697
9 Prochazka, K., Bednar, B., Svoboda, P., Trnena, J., Mukhtar, E. and Almgren, M. *J. Phys. Chem.* 1991, **85**, 4563

10 Heatly, F. and Begun, A. *Makromol Chem.* 1977, **178**, 1205
11 Spevacek, J. *J. Macromol. Chem., Rapid Commun.* 1982, **3**, 697
12 Candau, F., Heatly, F., Price, C. and Stubbersfield, R. B. *Eur. Polym. J.* 1984, **20**, 685
13 Bahadur, P. and Stastry, N. V. *J. Macromol. Sci.* 1986, **A23**, 1007
14 Ghiggino, K. P., Roberts, A. J. and Phillips, D. *Adv. Polym. Sci.* 1981, **40**, 69
15 Lakowicz, J. R. 'Principles of Fluorescence Spectroscopy', Plenum Press, New York, 1983
16 Fleming, G. R. 'Chemical Applications of Ultrafast Spectroscopy', Oxford University Press, New York, 1986
17 Major, M. D., Torkelson, J. M. and Brearley, A. M. *Macromolecules* 1990, **23**, 1700
18 Wilhelm, M., Zhao, C.-L., Wang, Y., Xu, R., Winnik, M. A., Mura, J.-L., Riess, G. and Croucher, M. D. *Macromolecules* 1991, **24**, 1033
19 Prochazka, K., Vajda, S., Fidler, V., Bednar, B., Mukhtar, E., Almgren, M. and Holmes, S. *J. Mol. Struct.* 1990, **219**, 337
20 Kiserow, D., Prochazka, K., Ramireddy, C., Tuzar, Z., Munk, P. and Webber, S. E. *Macromolecues* submitted
21 Campaigne, E. and Archer, W. L. *J. Am. Chem. Soc.* 1953, **75**, 989
22 Steward, F. H. C. *Aust. J. Chem.* 1953, **13**, 478
23 Pepper, K. V., Paisley, H. M. and Young, M. A. *J. Chem. Soc.* 1953, **IV**, 4097
24 Gibbson, H. W. and Bailey, F. C. *Macromolecules* 1976, **9**, 688
25 Tuzar, Z. and Kratochvil, P. *Collection Czech. Chem. Commun.* 1967, **32**, 3358
26 Gilbert, G. A. *Discuss. Faraday. Soc.* 1955, **20**, 68
27 Demas, J. N. 'Excited State Lifetime Measurements', Academic Press, New York, 1983
28 O'Connor, D. V. and Phillips, D. 'Time-Correlated Single Photon Counting', Academic Press, Florida, 1984
29 Cross, A. J. and Fleming, G. R. *Biophys. J.* 1984, **46**, 45
30 Levenberg, K. *Q. Appl. Math.* 1944, **2**, 164
31 Marquardt, D. W. *J. Soc. Ind. Appl. Math.* 1963, **11**, 431
32 Tuzar, Z., unpublished data
33 Pekan, O., Winnik, M. A. and Croucher, M. D. *Macromolecules* 1990, **23**, 2673
34 Michl, J. and Thulstrup, E. W. 'Spectroscopy with Polarized Light', VCH Publishers, New York, 1986
35 Johansson, L. B.-Å., Molotkovsky, J. G. and Bergelson, L. D. *Chem. Phys. Lipids* 1990, **53**, 185
36 von Jena, A. and Lessing, H. E. *Chem. Phys.* 1979, **40**, 245
37 Prochazka, K., Kiserow, D., Ramireddy, C., Munk, P. and Webber, S. E. in preparation
38 Gochanour, C. R., Andersen, H. C. and Fayer, M. D. *J. Chem. Phys.* 1979, **70**, 4254
39 Loring, R. F., Anderson, H. C. and Fayer, M. D. *J. Chem. Phys.* 1982, **76**, 2015
40 Loring, R. F. and Fayer, M. D. *Chem. Phys.* 1982, **70**, 139
41 Baumann, J. and Fayer, M. D. *J. Chem. Phys.* 1986, **85**, 4087
42 Fredrickson, G. H. and Frank, C. W. *Macromolecules* 1983, **16**, 1198
43 Fredrickson, G. H., Anderson, H. C. and Frank, C. W. *J. Chem. Phys.* 1983, **79**, 3572
44 Tuzar, Z., Plestil, J., Konak, C., Hlavata, D. and Sikora, A. *Makromol. Chem.* 1983, **184**, 2111
45 Berlman, I. B. in 'Energy Transfer Parameters of Aromatic Compounds', Academic Press, New York, 1973, p. 340
46 Semenov, A. N. *Sov. Phys. JETP* 1985, **61**, 733 (*Zh. Exp. Teor. Fiz.* 1985, **88**, 1242)
47 Rodrigues, K., Kausch, C. M., Kim, J., Quirk, R. P. and Mattice, W. L. *Polym. Bull.* 1991, **26**, 695
48 Rodrigues, K. and Mattice, W. L. *Polym. Bull.* 1991, **25**, 243
49 Cheng, P.-L., Berney, C. V. and Cohen, R. E. *Macromolecules* 1988, **21**, 3442